Characterization of blood coagulation dynamics and oxygenation in ex-vivo retinal vessels by fluorescence hyperspectral imaging

Originally published:

April 2020

Journal of Biophotonics 13(2020)8, e202000021

DOI: https://doi.org/10.1002/jbio.202000021

Characterization of blood coagulation dynamics and oxygenation in ex-vivo retinal vessels by fluorescence hyperspectral imaging (fHSI)

Rok Podlipec[1,2*], Zoran Arsov[1], Tilen Koklic[1], Janez Strancar[1*]

Jozef Stefan Institute, Condensed Matter Physics Department, Jamova cesta 39, 1000 Ljubljana, Slovenia
Helmholtz Zentrum Dresden Rossendorf, Ion Beam Center, Bautzner Landstrasse 400, 01328 Dresden, Germany
**Corresponding authors: rok.podlipec@ijs.si, janez.strancar@ijs.si*

Abstract

Blood coagulation mechanisms forming a blood clot and preventing hemorrhage have been extensively studied in the last decades. Knowing the mechanisms behind becomes very important particularly in the case of blood vessel diseases. Real-time and accurate diagnostics accompanied by the therapy are particularly needed for example in diseases related to retinal vasculature. In our study, we employ for the first time fluorescence hyperspectral imaging (fHSI) combined with the spectral analysis algorithm concept to assess physical as well as functional information of blood coagulation in real-time. By laser-induced local disruption of retinal vessels to mimic blood leaking and subsequent coagulation and a proper fitting algorithm, we were able to reveal and quantify the extent of local blood coagulation through direct identification of the change of oxyhemoglobin concentration within few minutes. We confirmed and illuminated the spatio-temporal evolution of the essential role of erythrocytes in the coagulation cascade as the suppliers of oxygenated hemoglobin. By additional optical tweezers force manipulation, we showed immediate aggregation of erythrocytes at the coagulation site. The presented fluorescence-based imaging concept could become a valuable tool in various blood coagulation diagnostics as well as theranostic systems if coupled with the laser therapy.

Keywords: Blood coagulation, hemoglobin oxygenation, fluorescence hyperspectral imaging, optical tweezers, comparative animal models, biomedical optics and biophotonics, diagnostics

1. Introduction

Blood coagulation or hemostasis has been extensively studied in the last 20 years [1]. The mechanisms and interdependent contributors for the clot formation starting from coagulation factors, platelets, prostaglandins, enzymes to proteins have well been known and are summarized in the ref. [2]. Tissue protective blood coagulation is divided into primary and secondary hemostasis. Primary encompasses vasoconstriction, platelet adhesion, its activation and aggregation forming “weak” interaction. Secondary encompasses triggered cascade of activated clotting factors to speed up thrombin and fibrin formation in order to create “strong” interaction and stabilize blood clot [3].

All gained knowledge of the mechanisms of blood coagulation is helping us to better understand and properly diagnose altered blood vessels in particular disorders. It is also important in the case of diagnostics of blood coagulation

This article has been accepted for publication and undergone full peer review but has not been through the copyediting, typesetting, pagination and proofreading process which may lead to differences between this version and the Version of Record. Please cite this article as doi:10.1002/jbio.202000021

dynamics when performing therapeutic targeted laser treatment. An example of such an application is diagnostics of altered vessels under the skin due to e.g. injuries or coagulation disorders or even diagnostics of altered vessels in eye retina due to e.g. diabetic retinopathy [4]. In order to effectively perform diagnostics of blood coagulation status or even real-time theranostics with accompanied pulsed targeted therapeutic laser system, techniques have to be capable of being applied *in-vivo* with enough sensitivity and specificity. Few advanced techniques have been lately developed which go towards this direction. One example is the assessment of blood coagulation by laser speckle rheology (LSR). The technique evaluates the viscoelastic properties of blood during coagulation by high-speed CMOS camera analysis of the rate of temporal speckle intensity fluctuations induced by coherent light [5]. Another example is real-time monitoring of the blood coagulation process by electrochemical sensing using electrical impedimetric imaging monitoring [6]. In one of the latest studies, optical coherence elastography (OCE) was implemented to analyze blood coagulation by monitoring viscosity properties through measurement of the attenuation coefficient of a compressional wave induced by a piezoelectric transducer [7]. In order to gather an accurate assessment of whole blood coagulation or hemostasis *ex-vivo*, microfluidic devices for automated monitoring [8] and microarray chips with microcantilevers for clot viscosity measurements [9] are being developed. The advantage of all mentioned techniques compared to conventional coagulation tests such as activated thromboplastin time (aPTT) or prothrombin time (PT) [10] is the ability to perform diagnostics in real-time at the *in-situ* point-of-care (POC). This is especially crucial in rapidly changing coagulation conditions in e.g. patients injured sites. What is common to all described techniques is that they are all successfully implemented *in-vitro* or *in-situ* mainly to diagnose whole blood coagulation abnormalities. Since the techniques are used to monitor perfused blood, one should search for new methods to study coagulation dynamics on injured vessel sites in a native environment *ex-vivo* or *in-vivo*.

To the best of our knowledge, there are very few studies that can track coagulation dynamics and its biochemical processes *in-vivo or ex-vivo* in real-time. One of the most promising techniques to perform such measurements of dynamics and localization of clot formation is based on fluorescence imaging. By pre-labeling of tissue factors and/or antibodies with fluorophores involved in clot formation, the techniques enable specific detection of constituents during thrombus development [11], [12]. Optical techniques based on scattered light or fluorescence detection undoubtedly show to be one of the most promising for *in-vivo* real-time imaging [13].

Optical based methods for studying hemoglobin properties have otherwise a long history. Properties such as oxygenation are typically measured by ratiometric analysis of optical densities of erythrocytes using specific optical band-pass filters at hemoglobin absorbance peaks [14] or with the accurate analysis of hemoglobin absorbance spectra [15]. A step further was to follow these properties at a microscopic level. The so-called microspectroscopic approach has been implemented in the studies of physiological and pathological processes in red blood cells [16], e.g. in the studies of hemoglobin component distribution [17] or hemoglobin kinetics of the reaction [18], by scanning

absorption-based micro-spectrophotometer on single cells. Besides absorbance, other spectroscopic modalities can be used as well. Recently, a multispectral imaging technique has been developed to study blood oxygenation in-vivo in animal models based on fluorescence detection [19]. Due to the collection of data in relatively wide spectral bands, the technique is limited to rather low spectral resolution. Improved multispectral imaging with up to ten narrower spectral bands was applied to study hemodynamics, mitochondrial metabolism and light scattering changes on rat model using optical intrinsic signal [20], while hyperspectral imaging with even more bands has been extensively used in medical research for tissue metabolic and hemodynamic monitoring [21]. However, methods based on scattered light have never been used for coagulation studies and lack sensitivity and specificity what could be achievable by fluorescence detection [22].

In the present study, we report the capability of fluorescence hyperspectral imaging (fHSI) combined with spectral analysis algorithm to resolve physical/morphological as well as biochemical/functional properties of blood coagulation at the targeted vessels in real-time exploiting auto-fluorescence of endogenous retinal fluorophores and if needed, the fluorescence of added contrast agent. The methodology concept presented here was developed in our lab to characterize and map local fluorophore environment changes at a microscopic level [23]. The advantage of our microspectroscopic approach is the accuracy of the determination of the fluorescence emission spectra and its peak with a nanometer resolution. In this work, our experimental approach has been modified in particular to distinguish between coagulated and non-coagulated blood by measuring oxyhemoglobin concentration. The role of erythrocytes and hemoglobin in blood clotting namely seems to be more important than previously thought [24]. One of the ways they influence blood clotting is through platelet activation by erythrocyte lysate containing extracellular hemoglobin, which lowers bioavailability of nitric oxide (NO) [25], an important cardiovascular signaling molecule and powerful vasodilator [26]. In the presented study we thus try to further elucidate the role of erythrocytes.

The microscope system was upgraded with appropriate pulsed ns diode laser to introduce local vessel injury in the retina and eyes were labeled with proper fluorophore just prior measurements to increase fluorescence contrast for fHSI measurements and to mimic human eye properties. Besides, optical tweezers (OT) [27] were added to the system to further characterize coagulation dynamics by optical trapping and manipulation of single erythrocytes or red blood cells (RBC) [28].

2. Materials and methods

To mimic *in-vivo* blood coagulation dynamics, measurements were performed on freshly enucleated *ex-vivo* porcine eyes gathered from a nearby slaughterhouse. Experiments were done on the intact retinal vessel in the whole porcine eyes to preserve the retinal tissue before testing. Porcine eyes were used due to their close similarities in the size as

well as the retinal vasculature and structure to the human eyes [29]. fHSI was additionally tested on relevant human retinal tissue of the enucleated patient's eye to test the suitability of the animal model. Due to the order of magnitude lower retinal auto-fluorescence in porcine eyes, fluorophore had to be injected locally to achieve similar fHSI contrast. Approval for work on human samples was granted by the Ethics Commission of the University Medical Centre, Ljubljana. Coagulation measurements using OT were followed on the dissected porcine retina using a high sub-micron magnification setup on an inverted confocal microscope system (Eclipse TE2000-E, Nikon).

2.1. Porcine eye sample preparation

2.1.1. Labeling of the intact eye retina

Fluorescence labeling of the retina was done after careful removal of cornea and lens (using surgical scissors and scalpel) (see Fig. 1A). Cornea and lens were gently removed to reduce inevitable optical aberration and to enable the implementation of standard microscope objectives. 100 µl of 10^{-5} M FITC solution in sterile phosphate buffer saline (PBS) was gently pipetted into the retinal tissue directly through the vitreous (Fig. 1A). The eye was transferred upside down onto a glass-bottom dish to perform measurements on the inverted microscope system.

2.1.2. Dissection of retina

Surgical scissors and a razor blade were used to cut the sclera on the eye equator. By shallow snipping motion, around the ball of an eye, sclera was split into two parts. Fresh retinal tissue was gently removed from the back part of an eye and placed onto a thin glass-bottom dish (Nunc™, Thermo Fisher) for high magnification/resolution measurements using a 60x water immersion objective with *NA* = 1.27 (Nikon).

2.2. Optical setup

Inverted confocal microscope system was upgraded with two optical modules, pulsed diode laser (Optotek Medical) and OT (Tweez 250Si, Aresis, Slovenia) (Fig. 1B, on the right). The first was used to induce efficient disruption of retinal vessels and the second to identify coagulation dynamics on clusters of erythrocytes. Neutral density (ND) filter and beam expander (both Thorlabs) were installed in the optical path of a pulsed laser to limit the power and dosage just enough to cause vessel injury and to fill the back aperture of the objective to achieve maximum beam focusing. Fluorescence excitation/emission module (BD CARV II, BD Biosciences, USA) complemented with 300W Xenon ARC lamp (Lambda LS, Sutter Instrument, Novato, CA), detection EMCCD cameras (iXon, Andor, UK; Rolera MGi Plus, Q-Imaging, Canada) and liquid crystal tunable filter LCTF (VariSpec, PerkinElmer, USA) (Fig. 1B, on the left)

were installed to acquire fluorescence spectra in each image pixel simultaneously as described in ref. [23]. Fluorescence excitation and emission are schematically presented with blue and green color, respectively. Pulsed diode and OT laser sources are shown in red and backside illumination in yellow. The latter was used for OT manipulation measurements of erythrocyte aggregation, where low signals (negative contrast) correspond to their density and the extent of coagulation.

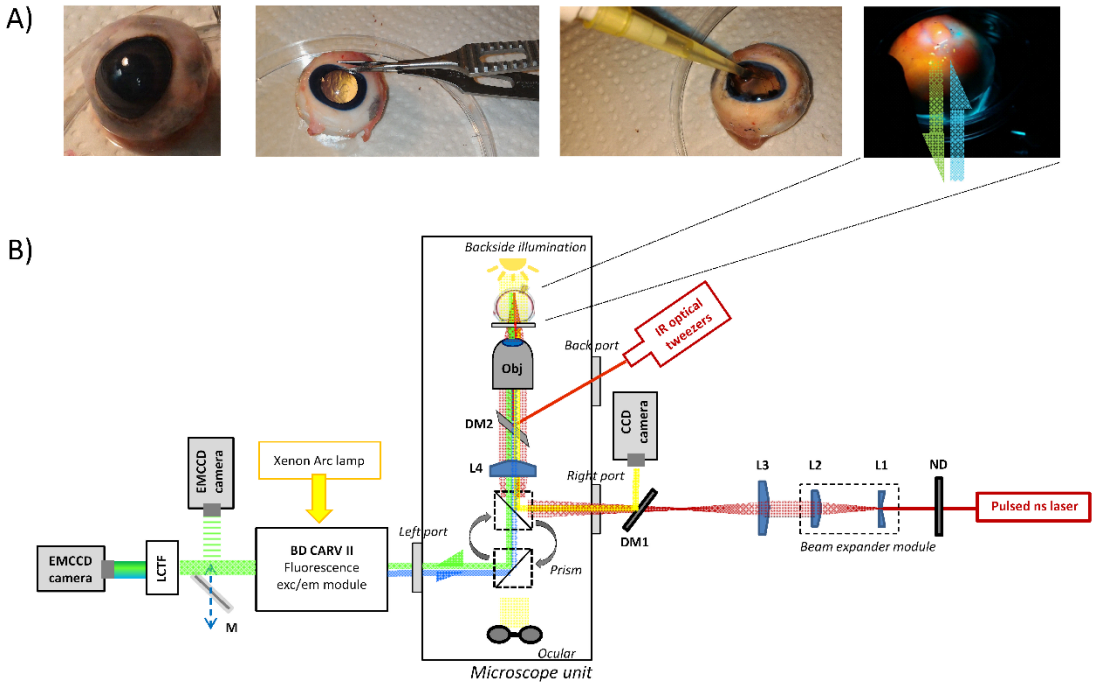

Fig. 1 Schematics of the experimental design with sample preparation (A) and optical setup (B). A) Sample preparation from left to right: freshly enucleated porcine eye, removal of cornea and lens, injection of FITC as a contrast agent and transfer of sample onto inverted microscope system followed by a typical blue light excitation (blue arrow) and green light emission (green arrow); B) experimental setup from left to right: Xenon Arc lamp in combination with confocal CARV II module composed of proper sets of excitation/dichroic/emission filters for an optimal fluorescence acquisition, backside illumination for an optimal identification of coagulating erythrocytes on the dissected retina, OT for force manipulation, pulsed ns diode laser for retinal vessels disruption and other components: EMCCD - Electron Multiplying Charge-Coupled Device; LCTF - Liquid Crystal Tunable Filter; M - mirror; DM - Dichroic Mirror; L – lens; ND – neutral density filter.

2.3. Disrupting retinal vessels

Intact retinal vessels of the fresh *ex-vivo* porcine eyes were locally disrupted by Nd:YAG pulsed diode laser source (E = 0.5 mJ, v = 5 Hz, t = 5ns, Optotek Medical). The same laser is being used in clinics for the treatment of posterior capsule opacification and was found capable of creating a photo-disruptive effect on the vessel wall as well. The

damage effect is however less localized and more energy is deposited to the tissue as compared to the femtosecond lasers sources [30] but is on the other hand much more cost-effective. The laser was focused through the pupil of an eye efficiently enough to disrupt the endothelial layer of the retinal vessel wall. Concurrent imaging was performed to locate, target and disrupt the vessel as well as to follow the leaking of the blood as depicted in Fig. 2. The images were taken using a 4X (*NA* = 0.1) and a 10X (*NA* = 0.3) magnification objectives (both Nikon), as presented in the top and bottom row, respectively. The acquired signal in the images originates from the autofluorescence of endogenous fluorophores, mainly from the retinal pigment epithelium (RPE) layer underneath [31], which is partially attenuated at hemoglobin sites due to its strong absorbance.

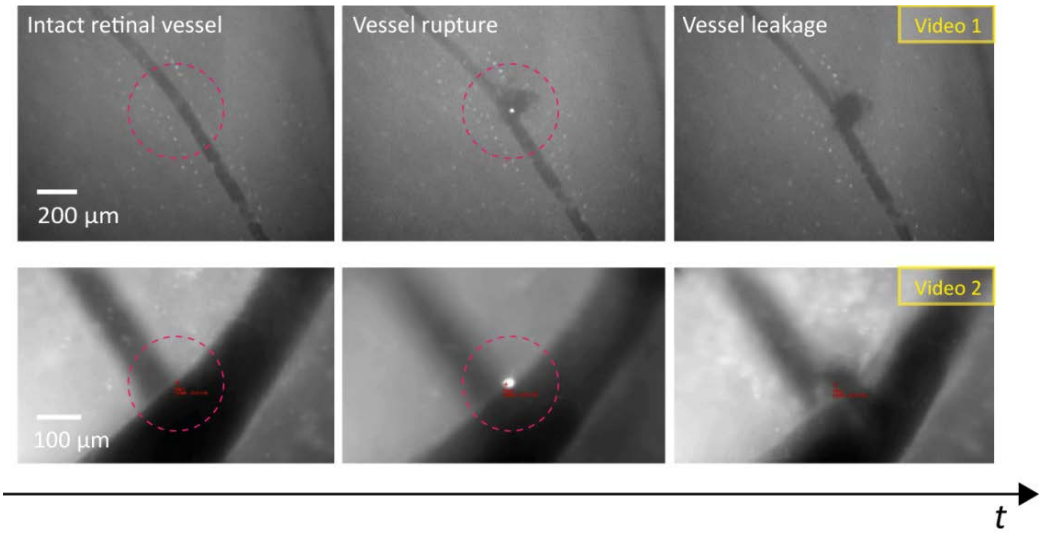

Fig. 2. Rupturing retinal vessel by focusing laser pulse on a vessel wall for retinal vessel coagulation studies performed on 4X (top row) and 10X (bottom row) objectives. Targeted spots are denoted with the dashed red circles. Blood leakage is seen immediately after vessel disruption (see Video 1 and Video 2 in Supporting Information). Contrast in acquired images was gained by auto-fluorescence signal of endogenous fluorescent molecules.

2.4. Fluorescence hyperspectral imaging and the algorithm for blood coagulation and oxygenation analysis

Targeted retinal spot was imaged using 4X and 10X objectives (both Nikon) and 300W Xenon Arc lamp excitation. An optimal set of excitation, dichroic and emission band-pass filters FF01-460/60, FF560-Di01 and FF01-550/88 (all Semrock, Rochester, NY) were chosen to properly excite and detect retinal fluorophore species. In the detected emission window hemoglobin most intensely absorb fluorescent light from the underneath RPE layer thus providing the highest negative contrast on the vessel site (Fig. 3A).

To characterize blood coagulation dynamics on the vessel leaking sites, fHSI was applied next. Spectral points were collected at a few nm steps by using a liquid crystal tunable filter (LCTF). With a recently developed algorithm for spectral fitting with sub-nm sensitivity for spectral changes [32], sub-nm differences of the spectral footprints at hemoglobin sites could potentially be detected.

The influence of spectral reshaping due to partial absorbance of underneath fluorescence on hemoglobin chromophores was first modeled on the known FITC fluorescence spectra (Fig. 3A). The evident spectral narrowing is shown on the right side which in principle can be quantified by fitting the parameter of spectral width *w*. However, the indirect biological meaning of the measured parameter for determining the extent of coagulation urged for the optimization. The new fitting algorithm, which we present in this study, gives us a direct measure of oxyhemoglobin concentration in blood. Furthermore, the reduction of oxyhemoglobin concentration on the coagulating region directly corresponds to the participation of erythrocytes in the coagulation pathway, which provides important functional information.

The change of fluorescence spectra on the vessel sites was fitted with the combination of two spectral components. The added second spectral component of oxyhemoglobin absorbance function (S_2) was subtracted from the first spectral component (S_1), the empirical asymmetric log-normal lineshape (LN) spectral model [32] as:

$$S_{\text{fit}}(\lambda; p_{1\_\text{backg}}, P_{2\_\text{HbO2}}) = P_{1\_\text{backg}}\, S_1(\lambda; \lambda_{\max}, w, a) - P_{2\_\text{HbO2}}\, S_2(\lambda) \quad (1)$$

An example of spectral fitting with the fitting curves S_1 and S_{fit} are shown at the bottom of Fig. 3B as dashed and continuous green curves, respectively. The proper parameters of the first fluorescence spectral component S_1, peak wavelength ($\lambda_{\max}$), spectral width (w) and spectral asymmetry (a) were determined from the background fluorescence spectra (see the blue squares in Fig. 3B) with nm accuracy. The remaining fitting parameters for the spectral analysis on the vessel sites were thus the portions of each spectral component, P_{1_backg} and P_{2_HbO2}, where $P_{2\_\text{HbO2}} = 1 - P_{1\_\text{backg}}$. P_{2_HbO2} gives the semi-quantitative information of oxyhemoglobin concentration and is the product of exact oxyhemoglobin concentration and the density of erythrocytes in the focal plane. If we assume the density remains constant, the change/decrease in P_{2_HbO2} directly indicates the change/decrease in oxyhemoglobin concentration. Relative change of blood oxygenation was thus measured on an injured vessel site.

Fitting of the experimental spectra ($S_{\text{exp}}(\lambda)$) was done by 3*3 image-pixel averaging to improve S/N followed by Nelder-Mead minimization method of the normalized χ^2 test to improve goodness of fit:

$$\chi^2 = \frac{\sum_{\lambda}(S_{fit}(\lambda) - S_{\text{exp}}(\lambda))^2}{N\sigma^2} \quad (2)$$

with σ as the standard deviation of a background signal. A threshold for the goodness of fit was set to $\chi^2 \leq 1$. To map only the vessel sites with the relevant oxyhemoglobin concentrations, the background fluorescence signal from the surrounding tissue was attenuated by multiplying each image pixel information with the high-pass filter in the form of $\exp(-(A/P_{2\_HbO2})^2)$. Constant A was chosen to attenuate the intensity in pixels with non-significant contributions of P_{2_HbO2} close to zero.

The fitting algorithm was first tested on fHSI of the intact porcine retina. Due to weak autofluorescence (AF) signal, originating mainly from the low lipofuscin concentration in the underneath RPE layer [33], there was not enough sensitivity to characterize oxygenation with the proposed model (Fig. 3B, left column). Weak AF signal can be probably ascribed to just a few month age of the enucleated eyes, since it is well-known that lipofuscin progressively accumulates in RPE with aging [34]. Another reason could be higher melanin content in porcine RPE compared to humans which can absorb more fluorescence light. To develop an animal model that would best mimic the auto-fluorescence properties of the relevant human retinal tissue, we performed the same fHSI experiment on the dissected human retina from an enucleated patient's eye. Approximately an order of magnitude higher auto-fluorescence provided high sensitivity for oxyhemoglobin characterization in the vessel (Fig. 3B, middle column). To induce similar sensitivity to oxyhemoglobin in model porcine eyes (Fig. 3B, right column), we injected an additional fluorescence probe into the retinal tissue. We have used few tens of µl of 10^{-5} M FITC solution gently injected into the retinal tissue.

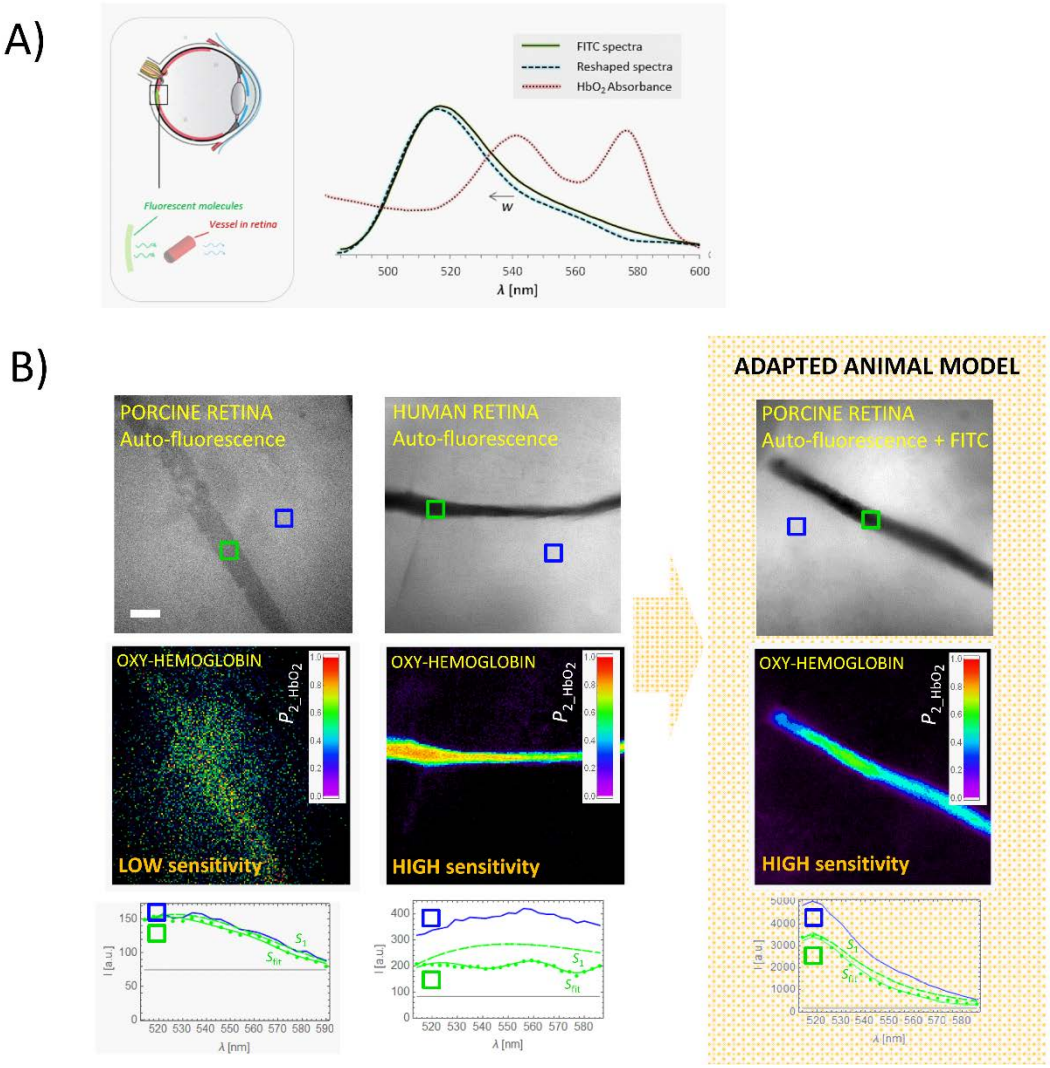

Fig. 3. Schematics of fHSI experiment and fluorescence spectra reshaping due to partial absorbance on hemoglobin molecules in retinal vessels using arbitrary data (FITC fluorescence, Invitrogen; HbO_2 absorbance spectra, *http://omlc.org/spectra/hemoglobin/*) (A) and the development of adapted animal model with high sensitivity to oxyhemoglobin inside vessels, comparable to relevant human retinal tissue (B). Fitted spectral curve (S_{fit}) obtained from the applied algorithm nicely fits the experimental spectral points, where S_1 was predefined by fitting the blue curve from the background fluorescence signal. Oxyhemoglobin maps are colour-coded with relative oxyhemoglobin concentration normalized to the region with maximum concentration. Scale bar is 100 μm.

2.5. Optical tweezers

Besides, blood coagulation at the leaking retinal vessel was characterized by OT force manipulation acting on single erythrocytes. OT, which has recently been shown powerful in the studies of erythrocytes aggregation [35] and

coagulation [28], was applied for the first time on *ex-vivo* intact tissue. To minimize the adverse effect of focused OT continuous-wave laser on retinal tissue (60x objective, *NA* = 1.27), the near-IR light source was used (λ = 1064 nm, Aresis, Slovenia). Using optical power of 300 mW few tens of pN forces were exerted on erythrocytes according to the ref. [35], [36]. The focal temperature increased for a few degrees due to local heating [37], still low enough not to trigger thermally induced blood coagulation. Trapping and manipulation of single erythrocytes were limited to the objective working distance of 170 µm. This required that retinal tissue was carefully removed from the back of an eye and transferred directly onto the pre-heated cover glass.

3. Results and discussion

3.1. Spatio-temporal fluorescence hyperspectral monitoring of localized blood coagulation and oxygenation in retinal vessels

After rupturing the vessel wall using an ns pulsed diode laser ($j = 3*10^{10}$ W/cm^2) directed through the eye pupil towards retinal tissue, fHSI was applied immediately to image the targeted site. Typical time-lapsed fluorescent images of blood outflow are presented in Fig. 4. The leakage from the right side (denoted with red arrow) significantly decreased after a few minutes, manifesting as a slow-down of blood cluster expansion outside the vessel (Fig. 4A). Through the fluorescence intensity, no information about coagulation or extension of clot formation could be acquired. The image analysis revealed only partial emptying of the vessels (above the dashed black curves, Figs. 4A and 4C), which means the number of absorbing hemoglobin or erythrocytes decreased inside the vessel due to their outflow. In contrast, oxyhemoglobin identification using fHSI and the fitting algorithm provided new insights into the clot formation (Fig. 4B). Using color-coding based on the portion of the fitted spectral component of the oxyhemoglobin, the local region of blood leakage where coagulation takes place can nicely be distinguished from non-coagulated blood inside the intact vessel region. Oxyhemoglobin concentration was found remarkably lower inside the region of a forming blood clot. The relative portion of oxyhemoglobin concentration dropped for at least 50% compared to the non-coagulated blood in the surrounding intact vessel. Relative intensity of oxyhemoglobin component in intact vessel $P_{2\_HbO2} = 0.6 \pm 0.1$ drops significantly to only $P_{2\_HbO2} = 0.2 \pm 0.1$ inside the blood clot. P_{2_HbO2} inside the vessel varies mostly due to the difference in local erythrocyte density in the focal volume. It has to be stressed though, that these values represent the relative change in oxyhemoglobin concentration not the absolute % of blood oxygenation, which in the scope of the study is not decisive. Fitting of the oxyhemoglobin parameter was done by minimization function χ^2 limited to 1, which gave the uncertainty of the parameter P_{2_HbO2} below 0.1 taking into account signal-to-noise-ratio

(SNR) of fluorescence data of 200 – 300. The uncertainty is notably less than the relative portion difference measured between the non-coagulated and coagulated region. Despite seemingly similar spectral curves on both regions (Fig. 4D), which is a consequence of strong fluorescence signal from the surrounding injected FITC, we could still nicely fit the oxyhemoglobin spectral component. In case of more distinguishable spectral differences, as observed in the experiment done on the human retina (Fig. 3B), which is due to better localization of auto-fluorescence in a thin underneath RPE layer, fitting could potentially be extended to quantify both oxy and deoxyhemoglobin.

The decrease in oxyhemoglobin concentration localized inside the blood clot confirms that blood coagulation immediately following the vessel-wall injury is a local process adjoined to the vessel wall which is in agreement with the known pathways of hemostasis [38]. Fig. 4B also shows that it does not lead to a complete vessel occlusion at the ruptured vessel site as the blood remains oxygenated (see the region under the blood clot). Thus, according to fHSI analysis, blood could still flow through the vessel. To confirm this, the second rupture was made on the vessel wall close to the coagulated site to induce secondary blood outflow (red arrow on Fig. 4C). Due to lower remaining pressure inside the vessel, blood outflow is less pronounced. The decrease of a fluorescence contrast inside the vessel (see the white arrows indicating shrinking of blood volume) additionally confirms the loss of the erythrocytes from the vessels, i.e. blood outflow. The experiments thus confirm the results from fHSI, which show not only the location and extent of blood coagulation but also the remaining blood functionality with the perfusion capability.

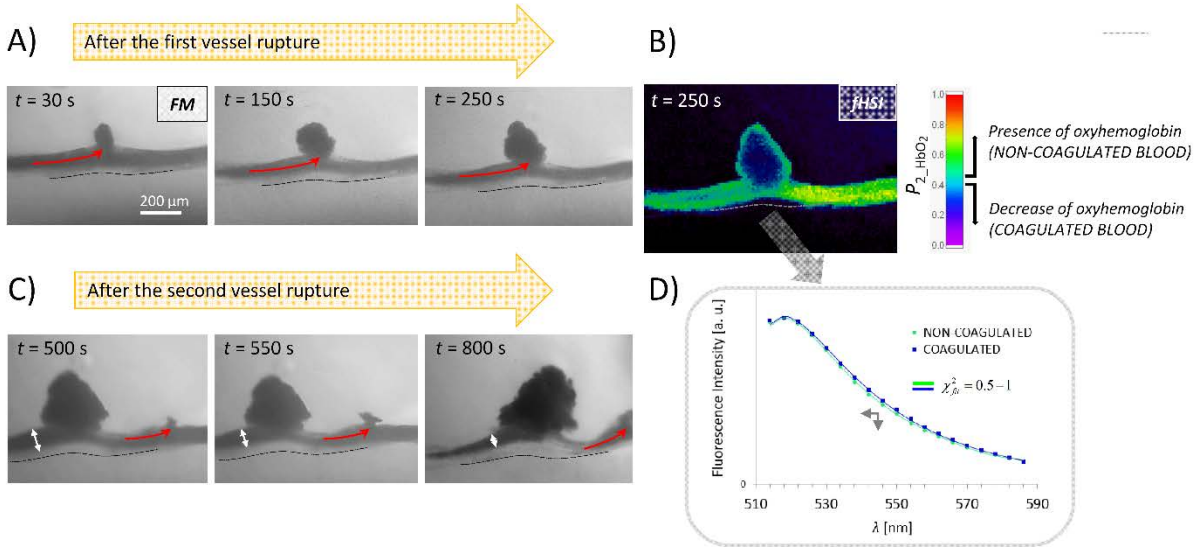

Fig. 4. Real-time measurement of retinal vessel leakage and coagulation after laser-induced vessel-wall damage by fluorescence microscopy (FM) (A) and fHSI (B). C) confirmation of remaining blood flow after primary clot formation; D) fitting the fluorescence spectra at the coagulated and non-coagulated site using spectral fitting algorithm. The spectral narrowing is more pronounced in non-coagulated blood (green color).

To gather more temporal information on coagulation dynamics, real-time imaging after vessel injury was performed next (Fig. 5). fHSI were taken at 0, 4, 12 and 18 minutes after rupturing the endothelial layer of a vessel wall. Expansion of a coagulated site into the region underneath the targeted vessel, which is towards the direction of detection, is evident. By measuring the change in the oxyhemoglobin concentration at the injured site, important details about the initial coagulation process have been gathered. A significant decrease in oxygenation is shown already in few minutes after vessel injury pointing on a fast, minute scale, active response of erythrocytes at the beginning of a clot formation. By releasing its hemoglobin to enhance platelet activation and its procoagulant activity [39], primary hemostasis takes place [2]. Namely, released oxyhemoglobin lowers or destroys NO bioavailability [26] through the de-oxygenation reaction in which NO reacts with oxyhemoglobin to form methemoglobin [25]. Tracking the changes in oxyhemoglobin concentration can thus directly point to physicochemical and biological changes of erythrocytes during coagulation.

From the time series, it is evident that the coagulated region slowly extends from the center of a blood clot towards the boundary of a hemorrhage region. After 20 minutes, there are very few regions left of oxygenated blood on the formed blood clot. Interestingly, it seems that very close to the perimeter of a blood clot no coagulation cascade is activated. A similar picture was seen by imaging different planes of the same blood clot (data not shown). According to one of the latest studies, this could be attributed to too low Ca^{2+} concentration in the perimeter of a blood clot to trigger the activation of coagulation [40]. Ca^{2+} from plasma has to be high enough to activate coagulation tissue factor, followed by a coagulation cascade.

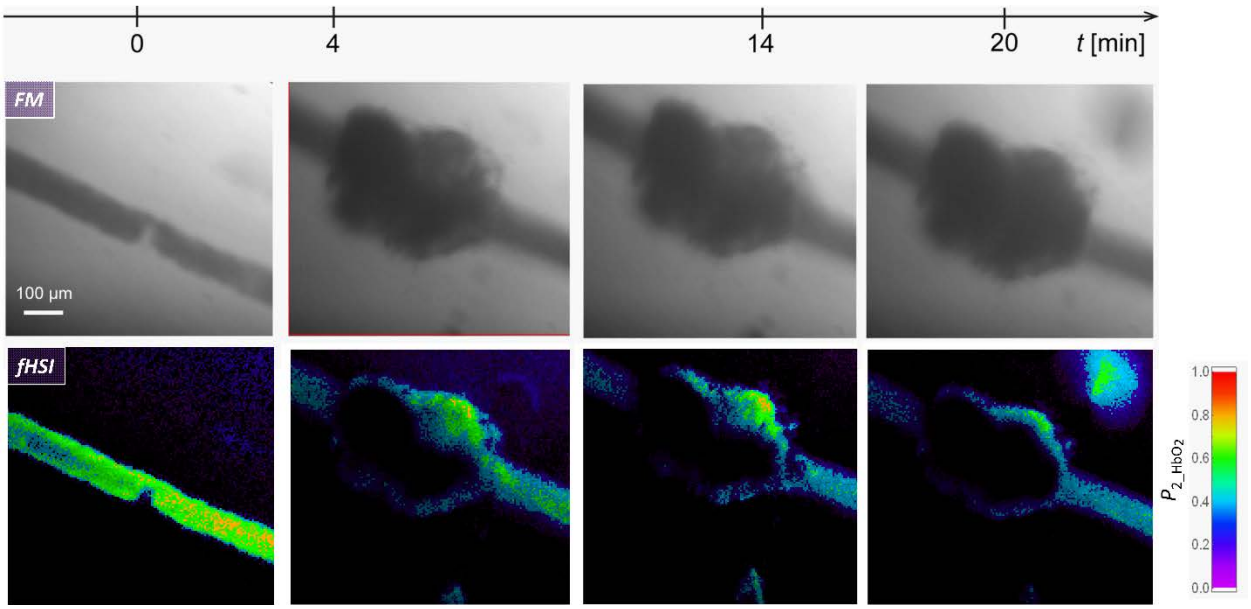

Fig. 5. Dynamics of retinal vessel coagulation measured by FM and fHSI. The later images are color-coded with the fitted portion of the second spectral component of oxyhemoglobin (P_{2_HbO2}).

Returning to the technical point of view, our described methodology could be discussed within a broader picture of the potential applications. Since no need for an additional contrast agent was shown by fHSI experiment done on highly auto-fluorescent human retinal tissue (Fig. 3B), the developed methodology could potentially be used for label-free diagnostics of retinal vessel diseases. However, one should take into account the non-uniformity of the background AF signal in the patients' eyes [41], thus expecting some lateral changes in spectral contrasts between the coagulated and the non-coagulated blood. The potential complementary imaging diagnostics technique to avoid this outcome could be based on the two-photon excitation (TPEF) imaging of erythrocytes involved in the coagulating region. This methodology, being continually developed throughout the last decade [42]–[44] could, besides detecting physical/morphological changes in hemoglobin distribution [44], exploit also the potential and relevant biochemical changes by fHSI.

The presented methodology could be applicable also for other eye-related diseases that show locally altered physicochemical and biological environments and could be thus inspected with our highly sensitive and specific fHSI. Additionally, it could be used to track chemical and structural changes in blood in case of applications of laser photocoagulation [45].

3.3. Monitoring retinal vessel coagulation dynamics on single erythrocytes using OT

To complement fHSI results and to gain additional insights into the blood clot formation in the seconds-time scale after vessel injury, OT was applied. However, the OT concept and the need for a high NA objective prevented the investigation of the intact eyes. Due to careful dissection of the whole retina from the back of an eye, coagulation measurement on the single-cell level was still feasible. Manipulation and force analysis of leaking and coagulating erythrocytes was enabled by the trapping power of OT localized on the cell periphery [28].

Some of the erythrocytes rapidly adhere to each other, manifesting as flowing aggregates (see Fig. 6, colored in green). The trapping force (red arrow) was exerted on pre-coagulating aggregate. The flow force of the leaking RBCs (orange arrow) was at one point too strong for the aggregate to remain inside the fixed trap (see the images at times 6s and 7s). However, the trapping force of few tens of pN was still strong enough to pull one erythrocyte from the aggregate. This means very few chemical bonds were established locally in this short time frame according to ref. [36]. If zoomed in, one can notice already formed “cross-bridges” between neighboring cells (see white arrow in the Inset image). Furthermore, we can nicely observe changed shape and thus mechanical properties of erythrocytes which were shown before with SEM [46]. This means that the initial coagulation process, which is localized at the damaged site close to the vessel wall, gets underway immediately after vessel rupture even in the studied *ex-vivo* retinal tissue. From the images, one cannot see the damaged retinal vessel directly since it lies above the focal plane region of leaking erythrocytes. For a detailed view of erythrocytes leakage and aggregation dynamics presented in Fig. 6 see Video 3 in Supporting Information.

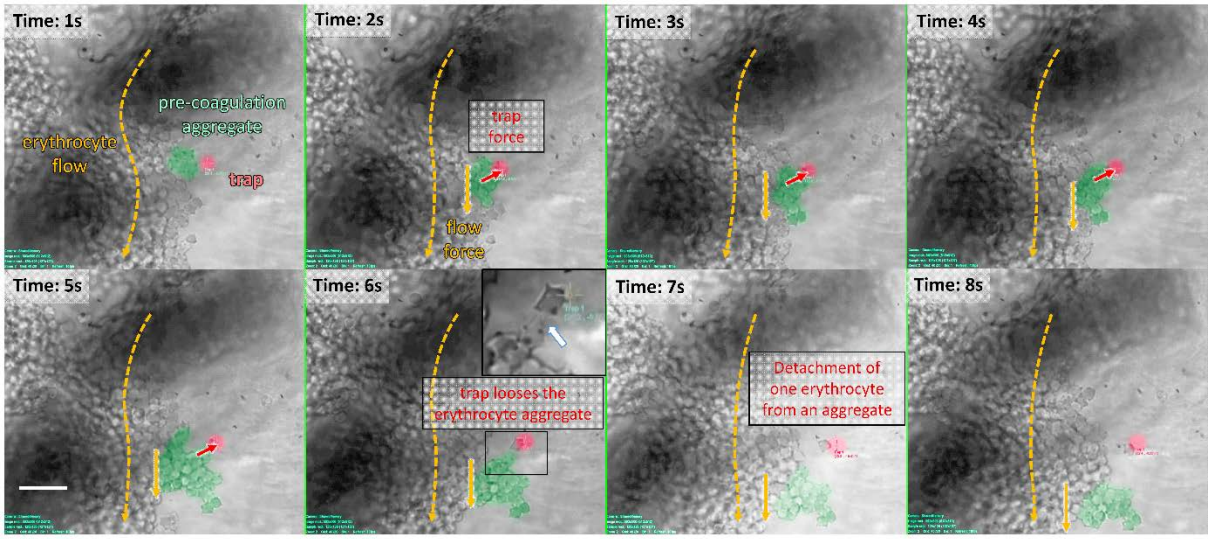

Fig. 6. Optical tweezers manipulation of erythrocytes leaking from a ruptured retinal vessel above the focal plane. Aggregated erythrocytes are represented with green color, the flow of erythrocyte with an orange color and an optical trap force with a red color. The image series represents the dynamics of the blood leakage and clot formation in the 8s interval. A zoomed image in the inset shows formed cross-bridges between individual erythrocytes (white arrow). Scale bar is 20 µm. For a detailed view of the experiment see Video 3 in Supporting Information.

Erythrocytes aggregation outside the ruptured spot was measured again after 10 minutes to analyze the development of blood coagulation. Almost all erythrocytes aggregated by forming densely packed clusters (see Fig. 7). Again OT was applied to measure forces and aggregation. Part of the cluster could still be moved with the force induced by optical tweezers of 100 pN (within the red dashed circle). For most parts OT force was not strong enough to move the aggregates, meaning that the aggregation/coagulation was too strong. By OT manipulation not only blood coagulation at the damaged site of a retinal vessel was confirmed, but it also provided more details on the dynamics of coagulation on a single erythrocyte level and is an added value to the results presented in Fig. 5 by fHSI. For a detailed view of force manipulation presented in Fig. 7 see Video 4 in Supporting Information.

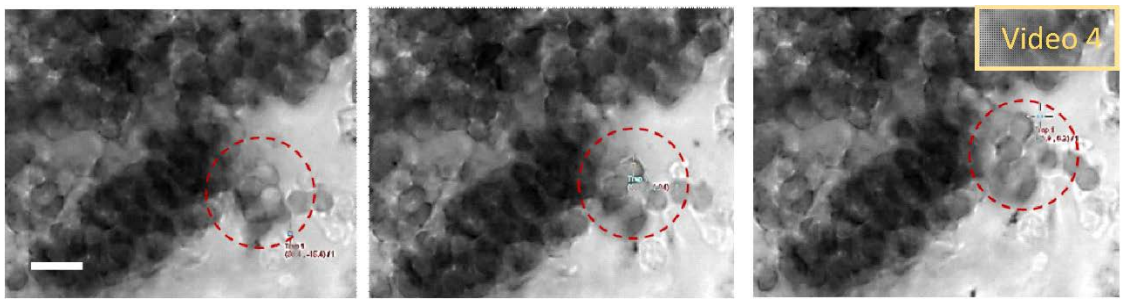

Fig. 7. OT manipulation of erythrocytes outside the ruptured retinal vessel 10 minutes after damage. The right part of the cluster could still be moved by OT force (within the red dotted circle). Scale bar is 10 µm. For a detailed view of the experiment see Video 4 in Supporting Information.

4. Conclusion

In this study fHSI, combined with a case-dependent fitting algorithm, was applied to identify a spatio-temporal evolution of blood coagulation in fresh *ex-vivo* retinal vessels. The capability of resolving nm spectral differences using the applied algorithm enabled us to detect small differences in optical properties of a forming blood clot. By direct fitting of the contribution of oxyhemoglobin absorbance spectral component on the fluorescence spectral information, we were able to quantify the relative change of blood oxygenation on the forming blood clot which reduces significantly inside a few minute timescale. The implemented methodology can provide new insights into physicochemical and biological aspects of the active role of the erythrocytes in the coagulation cascade, which has just recently been accepted. The same concept could be interesting also for label-free diagnostics, e.g. proliferative diabetic retinopathy with lots of leaking and coagulation of abnormal vessels. It can be applied as well for diagnosis or even theranostics of other eye-related diseases that introduce locally altered physico-chemical and biological environment detectable with sensitive and highly specific fHSI. By OT manipulation of single erythrocytes on blood coagulation site after laser-induced vessel injury, we additionally confirmed initiating coagulation events limited to the close vicinity of a vessel wall.

Funding and acknowledgments

This research work is supported by the Slovenian Research Agency (project L7-7561 and program P1-0060). The authors thank nearby slaughterhouse Loske mesnine d.o.o. to supply fresh porcine eyes and Optotek Medical for providing pulsed laser system. We would like to acknowledge also the group of prof. B. Drnovšek Olup on the Department of Ophthalmology of the University Medical Clinical Centre Ljubljana to provide us the access to the ex-

vivo sample of the retinal tissue. Special thanks go to dr. Iztok Urbančič for essential contribution in the spectral fitting algorithm.

No conflict of interest.

References

[1] M. Hoffman and D. M. Monroe, "A cell-based model of hemostasis," *Thromb. Haemost.*, vol. 85, no. 6, pp. 958–965, Jun. 2001.

[2] C. Garmo and B. Burns, "Physiology, Clotting Mechanism," in *StatPearls*, Treasure Island (FL): StatPearls Publishing, 2019.

[3] A. J. Gale, "Current Understanding of Hemostasis," *Toxicol. Pathol.*, vol. 39, no. 1, pp. 273–280, 2011, doi: 10.1177/0192623310389474.

[4] N. Relhan and H. W. Flynn, "The Early Treatment Diabetic Retinopathy Study historical review and relevance to today's management of diabetic macular edema," *Curr. Opin. Ophthalmol.*, vol. 28, no. 3, pp. 205–212, May 2017, doi: 10.1097/ICU.0000000000000362.

[5] M. M. Tripathi, Z. Hajjarian, E. M. Van Cott, and S. K. Nadkarni, "Assessing blood coagulation status with laser speckle rheology," *Biomed. Opt. Express*, vol. 5, no. 3, pp. 817–831, Feb. 2014, doi: 10.1364/BOE.5.000817.

[6] K. F. Lei, K.-H. Chen, P.-H. Tsui, and N.-M. Tsang, "Real-Time Electrical Impedimetric Monitoring of Blood Coagulation Process under Temperature and Hematocrit Variations Conducted in a Microfluidic Chip," *PLoS ONE*, vol. 8, no. 10, Oct. 2013, doi: 10.1371/journal.pone.0076243.

[7] X. Xu, J. Zhu, J. Yu, and Z. Chen, "Viscosity monitoring during hemodiluted blood coagulation using optical coherence elastography," *IEEE J. Sel. Top. Quantum Electron. Publ. IEEE Lasers Electro-Opt. Soc.*, vol. 25, no. 1, Feb. 2019, doi: 10.1109/JSTQE.2018.2833455.

[8] A. Jain, A. Graveline, A. Waterhouse, A. Vernet, R. Flaumenhaft, and D. E. Ingber, "A shear gradient-activated microfluidic device for automated monitoring of whole blood haemostasis and platelet function," *Nat. Commun.*, vol. 7, p. 10176, Jan. 2016, doi: 10.1038/ncomms10176.

[9] F. Padovani, J. Duffy, and M. Hegner, "Nanomechanical clinical coagulation diagnostics and monitoring of therapies," *Nanoscale*, vol. 9, no. 45, pp. 17939–17947, Nov. 2017, doi: 10.1039/c7nr06992h.

[10] H. Saito, T. Matsushita, and T. Kojima, "Historical perspective and future direction of coagulation research," *J. Thromb. Haemost. JTH*, vol. 9 Suppl 1, pp. 352–363, Jul. 2011, doi: 10.1111/j.1538-7836.2011.04362.x.

[11] S. Falati, P. Gross, G. Merrill-Skoloff, B. C. Furie, and B. Furie, "Real-time in vivo imaging of platelets, tissue factor and fibrin during arterial thrombus formation in the mouse," *Nat. Med.*, vol. 8, no. 10, pp. 1175–1181, Oct. 2002, doi: 10.1038/nm782.

[12] B. C. Cooley, "In vivo fluorescence imaging of large-vessel thrombosis in mice," *Arterioscler. Thromb. Vasc. Biol.*, vol. 31, no. 6, pp. 1351–1356, Jun. 2011, doi: 10.1161/ATVBAHA.111.225334.

[13] A. S. Luthman, S. Dumitru, I. Quiros-Gonzalez, J. Jose ph, and S. E. Bohndiek, "Fluorescence hyperspectral imaging (fHSI) using a spectrally resolved detector array," *J. Biophotonics*, vol. 10, no. 6–7, pp. 840–853, Jun. 2017, doi: 10.1002/jbio.201600304.

[14] C. G. Ellis, M. L. Ellsworth, and R. N. Pittman, "Determination of red blood cell oxygenation in vivo by dual video densitometric image analysis," *Am. J. Physiol.-Heart Circ. Physiol.*, vol. 258, no. 4, pp. H1216–H1223, Apr. 1990, doi: 10.1152/ajpheart.1990.258.4.H1216.

[15] S. Frische, S. Bruno, A. Fago, R. E. Weber, and A. Mozzarelli, "Oxygen binding by single red blood cells from the red-eared turtle Trachemys scripta," *J. Appl. Physiol. Bethesda Md 1985*, vol. 90, no. 5, pp. 1679–1684, May 2001, doi: 10.1152/jappl.2001.90.5.1679.
[16] M. Brunori, M. Coletta, A. Bellelli, V. Evangelista, P. A. Benedetti, and M. Brumen, "Microspectroscopy of red blood cells," *Haematologia (Budap.)*, vol. 22, no. 2, pp. 69–78, 1989.
[17] M. Brunori, B. Giardina, E. Antonini, P. A. Benedetti, and G. Bianchini, "Distribution of the haemoglobin components of trout blood among the erythrocytes: Observations by single-cell spectroscopy," *J. Mol. Biol.*, vol. 86, no. 1, pp. 165–169, Jun. 1974, doi: 10.1016/S0022-2836(74)80015-X.
[18] M. Coletta, B. Giardina, G. Amiconi, P. Gualtieri, P. A. Benedetti, and M. Brunori, "Kinetics of the reaction of intraerythrocytic haemoglobin by single cell microspectroscopy: effect of shape and osmolarity," *FEBS Lett.*, vol. 190, no. 2, pp. 217–220, Oct. 1985, doi: 10.1016/0014-5793(85)81287-4.
[19] M. B. Bouchard, B. R. Chen, S. A. Burgess, and E. M. C. Hillman, "Ultra-fast multispectral optical imaging of cortical oxygenation, blood flow, and intracellular calcium dynamics," *Opt. Express*, vol. 17, no. 18, pp. 15670–15678, Aug. 2009.
[20] C. Yin, F. Zhou, Y. Wang, W. Luo, Q. Luo, and P. Li, "Simultaneous detection of hemodynamics, mitochondrial metabolism and light scattering changes during cortical spreading depression in rats based on multi-spectral optical imaging," *NeuroImage*, vol. 76, pp. 70–80, Aug. 2013, doi: 10.1016/j.neuroimage.2013.02.079.
[21] L. Giannoni, F. Lange, and I. Tachtsidis, "Hyperspectral imaging solutions for brain tissue metabolic and hemodynamic monitoring: past, current and future developments," *J. Opt. 2010*, vol. 20, no. 4, Apr. 2018, doi: 10.1088/2040-8986/aab3a6.
[22] J. R. Lakowicz, Ed., "Fluorescence Sensing," in *Principles of Fluorescence Spectroscopy*, Boston, MA: Springer US, 2006, pp. 623–673.
[23] Z. Arsov *et al.*, "Fluorescence microspectroscopy as a tool to study mechanism of nanoparticles delivery into living cancer cells," *Biomed. Opt. Express*, vol. 2, no. 8, pp. 2083–2095, Aug. 2011, doi: 10.1364/BOE.2.2083.
[24] J. W. Weisel and R. I. Litvinov, "Red blood cells: the forgotten player in hemostasis and thrombosis," *J. Thromb. Haemost. JTH*, vol. 17, no. 2, pp. 271–282, 2019, doi: 10.1111/jth.14360.
[25] M. P. Doyle and J. W. Hoekstra, "Oxidation of nitrogen oxides by bound dioxygen in hemoproteins," *J. Inorg. Biochem.*, vol. 14, no. 4, pp. 351–358, Jan. 1981, doi: 10.1016/S0162-0134(00)80291-3.
[26] C. C. Helms *et al.*, "Mechanisms of hemolysis-associated platelet activation," *J. Thromb. Haemost. JTH*, vol. 11, no. 12, pp. 2148–2154, Dec. 2013, doi: 10.1111/jth.12422.
[27] A. Ashkin, J. M. Dziedzic, J. E. Bjorkholm, and S. Chu, "Observation of a single-beam gradient force optical trap for dielectric particles," *Opt. Lett.*, vol. 11, no. 5, p. 288, May 1986, doi: 10.1364/ol.11.000288.
[28] B.-W. Yang and Z. Li, "Measuring micro-interactions between coagulating red blood cells using optical tweezers," *Biomed. Opt. Express*, vol. 1, no. 4, pp. 1217–1224, Oct. 2010, doi: 10.1364/BOE.1.001217.
[29] I. Sanchez, R. Martin, F. Ussa, and I. Fernandez-Bueno, "The parameters of the porcine eyeball," *Graefes Arch. Clin. Exp. Ophthalmol. Albrecht Von Graefes Arch. Klin. Exp. Ophthalmol.*, vol. 249, no. 4, pp. 475–482, Apr. 2011, doi: 10.1007/s00417-011-1617-9.
[30] N. Nishimura, C. B. Schaffer, and D. Kleinfeld, "In vivo manipulation of biological systems with femtosecond laser pulses," in *High-Power Laser Ablation VI*, 2006, vol. 6261, p. 62611J, doi: 10.1117/12.668886.
[31] S. Schmitz-Valckenberg, F. G. Holz, A. C. Bird, and R. F. Spaide, "Fundus autofluorescence imaging: review and perspectives," *Retina Phila. Pa*, vol. 28, no. 3, pp. 385–409, Mar. 2008, doi: 10.1097/IAE.0b013e318164a907.
[32] I. Urbančič, Z. Arsov, A. Ljubetič, D. Biglino, and J. Strancar, "Bleaching-corrected fluorescence microspectroscopy with nanometer peak position resolution," *Opt. Express*, vol. 21, no. 21, pp. 25291–25306, Oct. 2013, doi: 10.1364/OE.21.025291.

[33] A. D. Marmorstein, L. Y. Marmorstein, H. Sakaguchi, and J. G. Hollyfield, "Spectral profiling of autofluorescence associated with lipofuscin, Bruch's Membrane, and sub-RPE deposits in normal and AMD eyes," *Invest. Ophthalmol. Vis. Sci.*, vol. 43, no. 7, pp. 2435–2441, Jul. 2002.
[34] C. J. Kennedy, P. E. Rakoczy, and I. J. Constable, "Lipofuscin of the retinal pigment epithelium: a review," *Eye Lond. Engl.*, vol. 9 (Pt 6), pp. 763–771, 1995, doi: 10.1038/eye.1995.192.
[35] K. Lee *et al.*, "Optical tweezers study of red blood cell aggregation and disaggregation in plasma and protein solutions," *J. Biomed. Opt.*, vol. 21, no. 3, p. 35001, Mar. 2016, doi: 10.1117/1.JBO.21.3.035001.
[36] R. Podlipec and J. Štrancar, "Cell-scaffold adhesion dynamics measured in first seconds predicts cell growth on days scale – optical tweezers study," *ACS Appl. Mater. Interfaces*, vol. 7, no. 12, pp. 6782–6791, Apr. 2015, doi: 10.1021/acsami.5b00235.
[37] E. J. G. Peterman, F. Gittes, and C. F. Schmidt, "Laser-Induced Heating in Optical Traps," *Biophys. J.*, vol. 84, no. 2, pp. 1308–1316, Feb. 2003.
[38] K. G. Mann, T. Orfeo, S. Butenas, A. Undas, and K. Brummel-Ziedins, "Blood Coagulation Dynamics in Hemostasis," *Hamostaseologie*, vol. 29, no. 1, pp. 7–16, Jan. 2009.
[39] E. M. Bevers, P. Comfurius, and R. F. Zwaal, "Platelet procoagulant activity: physiological significance and mechanisms of exposure," *Blood Rev.*, vol. 5, no. 3, pp. 146–154, Sep. 1991, doi: 10.1016/0268-960x(91)90031-7.
[40] T. Koklic, R. Majumder, and B. R. Lentz, "Ca2+ switches the effect of PS-containing membranes on Factor Xa from activating to inhibiting: implications for initiation of blood coagulation," *Biochem. J.*, vol. 462, no. 3, pp. 591–601, Sep. 2014, doi: 10.1042/BJ20140130.
[41] S. Vujosevic, M. Casciano, E. Pilotto, B. Boccassini, M. Varano, and E. Midena, "Diabetic macular edema: fundus autofluorescence and functional correlations," *Invest. Ophthalmol. Vis. Sci.*, vol. 52, no. 1, pp. 442–448, Jan. 2011, doi: 10.1167/iovs.10-5588.
[42] D. Li *et al.*, "Time-resolved detection enables standard two-photon fluorescence microscopy for in vivo label-free imaging of microvasculature in tissue," *Opt. Lett.*, vol. 36, no. 14, pp. 2638–2640, Jul. 2011, doi: 10.1364/OL.36.002638.
[43] G. Palczewska *et al.*, "Noninvasive two-photon microscopy imaging of mouse retina and retinal pigment epithelium through the pupil of the eye," *Nat. Med.*, vol. 20, no. 7, pp. 785–789, Jul. 2014, doi: 10.1038/nm.3590.
[44] K. Bukara *et al.*, "Mapping of hemoglobin in erythrocytes and erythrocyte ghosts using two photon excitation fluorescence microscopy," *J. Biomed. Opt.*, vol. 22, no. 2, p. 26003, 01 2017, doi: 10.1117/1.JBO.22.2.026003.
[45] J. F. Black and J. K. Barton, "Chemical and structural changes in blood undergoing laser photocoagulation," *Photochem. Photobiol.*, vol. 80, pp. 89–97, Aug. 2004, doi: 10.1562/2004-03-05-RA-102.1.
[46] D. B. Cines *et al.*, "Clot contraction: compression of erythrocytes into tightly packed polyhedra and redistribution of platelets and fibrin," *Blood*, vol. 123, no. 10, pp. 1596–1603, Mar. 2014, doi: 10.1182/blood-2013-08-523860.